THE JOHNS HOPKINS UNIVERSITY

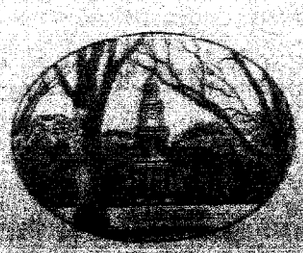

DEPARTMENT OF PHYSICS

TECHNICAL REPORT NO. 3

N. A. S. A. Research Grant NsG193-62

INSTRUMENTATION FOR
FAR ULTRAVIOLET
ROCKET SPECTROPHOTOMETRY

by

Wm. G. Fastie

AUGUST, 1963

Baltimore 18, Maryland

TECHNICAL REPORT
No. 3

INSTRUMENTATION FOR FAR ULTRAVIOLET ROCKET SPECTROPHOTOMETRY

Wm. G. Fastie
The Johns Hopkins University
Baltimore 18, Maryland

NASA RESEARCH GRANT
NsG 193-62

Prepared for

NATIONAL AERONAUTICS AND SPACE ADMINISTRATION
Washington, D. C.
August, 1963

Instrumentation for Far Ultraviolet Rocket Spectrophotometry

I. Introduction

The measurement of light emission in the upper atmosphere of the earth below 3000 A can be accomplished at altitudes presently available only to rockets and satellites because of the opacity of ozone in the region 3000 to 2000 A and of oxygen at shorter wavelengths. The upper atmospheric processes of chemiluminescence, dissociation, electrical discharge, resonance radiation, and fluorescence all produce emission in the region below 3000 A. In particular, most of the resonance lines of atmospheric species lie below 3000 A, and a measure of these emissions can be very valuable in determining the atmospheric structure.

Of greater importance is the fact that the physical conditions existing in the upper atmosphere cannot be reproduced in the laboratory because of dimensional limitations, and thus the techniques described herein permit basic measurements of interactions between photons, ions, atoms and molecules which we have no other means of observing.

II. Limitations on Instrument Sensitivity

The signal from a radiating source which can be delivered to a detector (Fig. 1) is given by the radiometer formula

$$S = B_S^{\lambda} \, d\lambda \, \frac{A_S \, A_c \, T}{d^2} \qquad (1)$$

where B_S^{λ} is the brightness of a continuous source per steradian at wavelength λ in the wavelength interval $d\lambda$

A_S is the area of the source

A_c is the area of the collector

d is the distance between the source and the collector

T is the transmission of the spectrometer

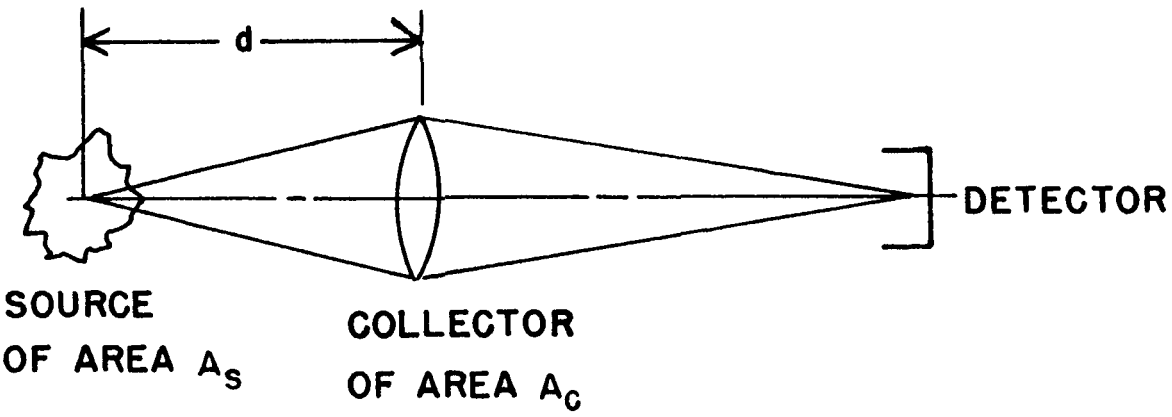

Fig. 1. Radiometer Geometry

If the energy relationship of Eq. (1) is applied to a spectrophotometer, the source area becomes the effective area of the entrance slit, i.e. the product of the slit length L and the slit width W, the collector area becomes the projected area of the grating, i.e. $A_g \cos \theta$, where θ is the angle of incidence or diffraction, so d becomes the focal length F of the spectrometer, and the relationship between the spectral band pass $d\lambda$ and the slit width W in a Littrow grating spectrophotometer is

$$W = \frac{2F\, d\lambda \tan \theta}{\lambda} \tag{2}$$

as determined by the diffraction grating formula. Eq. (1) can thus be written

$$S = 2 \frac{B_\lambda^S}{\lambda}\, d\lambda^2\, A_g \frac{L}{F} \sin \theta\, T. \tag{3}$$

where L is the slit length

A_g is the area of the ruled surface of the grating

θ is the angle at which the grating is used

F is the focal length of the spectrophotometer

It should be noted that the signal varies as the square of the spectral pass band only for a continuous source. For a line source where the line width is small compared to the spectral slit width, B_λ^S is inversely proportional to $d\lambda$ and the signal strength then varies linearly with $d\lambda$.

It is important to note that the only three geometrical parameters which affect the throughput of the spectrophotometer are the ratio of the slit length to focal length (L/F), the actual area of the grating (A_g) and the angle at which the grating is used (0). It is possible to rewrite Eq. (3) to include the focal ratio or f number of the system, for example

$$S = \frac{L\sqrt{A_g} \sin \theta\, T}{f} \tag{4}$$

but it should be noted that Eq. (4) expresses the geometrical parameters in a manner which confuses the issue. The slit length and the f number are not independent parameters, whereas the angular length of the slit (L/F) has a constant value for a given system independent of f number, and dependent only on the aberrations and image-forming properties of the particular optical system. Eq. (3) thus properly separates the geometrical parameters and demonstrates that a photospectrophotometer has quite different geometrical properties than a photographic spectrograph where the sensitivity is directly dependent on the f value.

It should also be noted that Eq. (3) shows that the signal can be increased by using the grating at a high angle (θ). The sin θ factor arises from the fact that the projected area of the grating decreases with θ (varying as the cosine), but the spectral dispersion increases as tan θ, thus permitting wider slits at larger values of θ, the combined effect of the grating angle being then proportional to the sine of the angle. In order to work at very short wavelengths with a large grating angle, and avoid overlapping orders, it is necessary to employ gratings with very fine rulings. We have used gratings ruled with 90,000 lines/inch. These gratings have the additional advantage of appearing to be mirrors for visible radiation, and thus scatter much less long-wavelength solar radiation than coarser gratings.

A scale drawing of the optical layout of the flight spectrometer is shown in Fig. 2. With the dimensions shown in Fig. 2, and with the following values for the instrument which correspond to actual flight conditions, $A_S = 1.5$ sq.cm., $A_c = 100$ sq.cm., $T = 0.2$, $B_S^{\lambda}\, d\lambda = 1/4\pi \times 10^6$ photons/ster/sec., $F = 50$ cm., Eq. (1) gives

$$S = 10^3 \text{ photons/sec.} \tag{5}$$

The value used for $B_S^{\lambda}\, d\lambda$ is the photon unit called a Rayleigh, which is defined as 10^6 photons/sec/cm^2 emitted over an entire hemisphere. In the case of Rayleigh scattering or any other continuous source, the value of B_S^{λ} depends on the spectral pass band of the equipment, but for narrow line emission, $B_S^{\lambda}\, d\lambda$ is independent of the spectrometer pass band.

Photomultiplier tubes for the spectral region 1000 to 3000 A can now be obtained with photocathodes such as CsTe and CsI which have high work functions, therefore, low dark current and insensitivity to long wavelength solar radiation, which can be a problem as a scatter signal in far U. V. spectrometers. These detectors have a quantum efficiency of about 10%. Thus the signal of Eq. (5) becomes only 100 photoelectrons/sec/Rayleigh. The dark current of the detectors can be as small as ten false electrons/sec, and the lower limit of 1 Rayleigh is an easily achievable goal if one second of observation time is available.

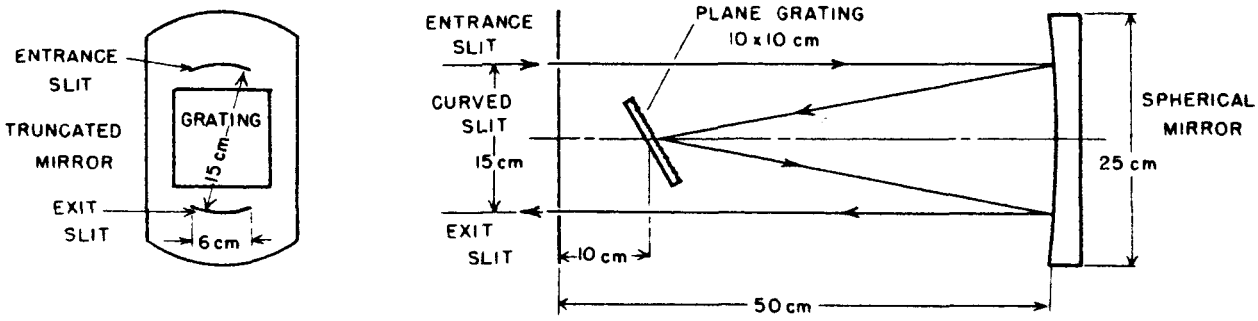

Fig. 2. Optical Layout of Flight Spectrophotometer

III. Description of Flight Spectrometer

The Ebert optical system shown in Fig. 2 has the capability of extremely high spectral resolution and high radiant throughput. These properties have been previously described [1,2,3] and the signal calculation of Sec. II emphasizes the energy-gathering capability of the flight system. A most important feature of the system for rocket applications is its compactness and its extreme ruggedness. This point is illustrated in Fig. 3, which shows the optical components in a conical housing mounted in a nose cone. All of the electronic components (high voltage supply, photomultiplier tubes, and amplifiers) are mounted in the detector housing which contains the far U. V. tube at the exit slit plus three photomultiplier tubes, with interference filters and baffles for measurements of selected visible and ultraviolet spectral bands. The power for operating the electronics and for driving the wavelength scan motor is supplied by rechargeable nickel-cadmium batteries attachted to the side of the main magnesium casting. There are six baffled holes in the main casting for quick removal of air when the nose tip is ejected after rocket burnout. The output of the amplifiers is fed to the telemetry equipment, which is located in the top end of the rocket. The entire spectrometer assembly, including detector housing, baffles, and battery power supply, weighs 35 pounds. Fig. 4 is a photograph of a flight ready instrument.

The manner in which the Ebert mirror is mounted in the casting is shown in Fig. 5. The mirror blank has holes sand-blasted in its rear surface for weight reduction, and has a flat annulus ground on its front edge. Three-point support on this flat and at opposite points on the rear surface provide positioning for the mirror, and six points of support on the mirror edge firmly lock the mirror. All supports of the mirror are nylon-tipped steel screws or pins. The grating is similarly held in a box on the grating shaft which rotates in ball bearings mounted in the top and bottom of the main casting.

Precision machining of the spectrometer casting and of the mirror positioning pins, and close tolerances on the radius of curvature of the spherical mirror are maintained, with the result that the instrument when assembled is automatically in adequate optical adjustment to provide a spectral resolution of less than two Angstrom units, well below the resolution requirements of experiments we have performed to date. Adjustment of the grating is necessary, but can be accomplished in the grating box subassembly on an optical bench prior to installation in the main casting.

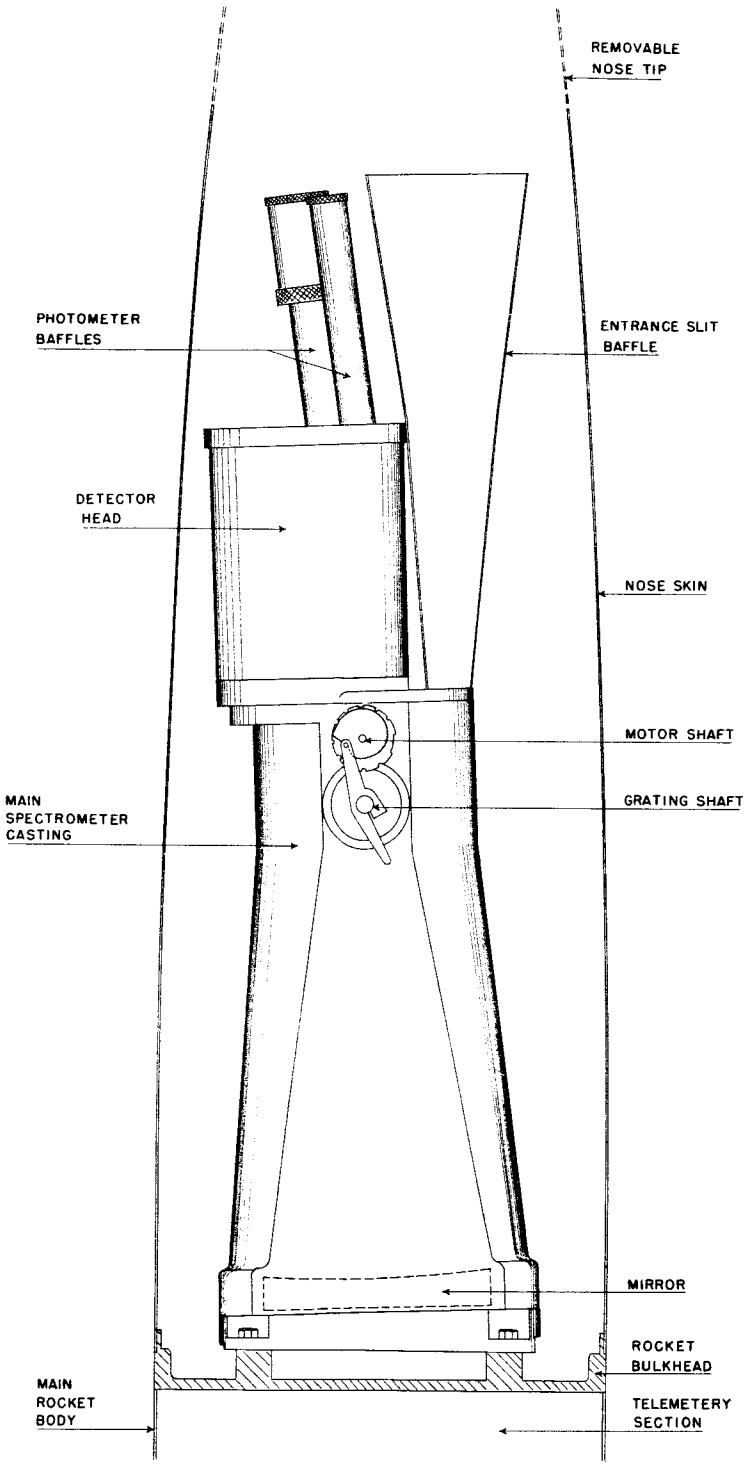

Fig. 3. Nose Cone Mounting

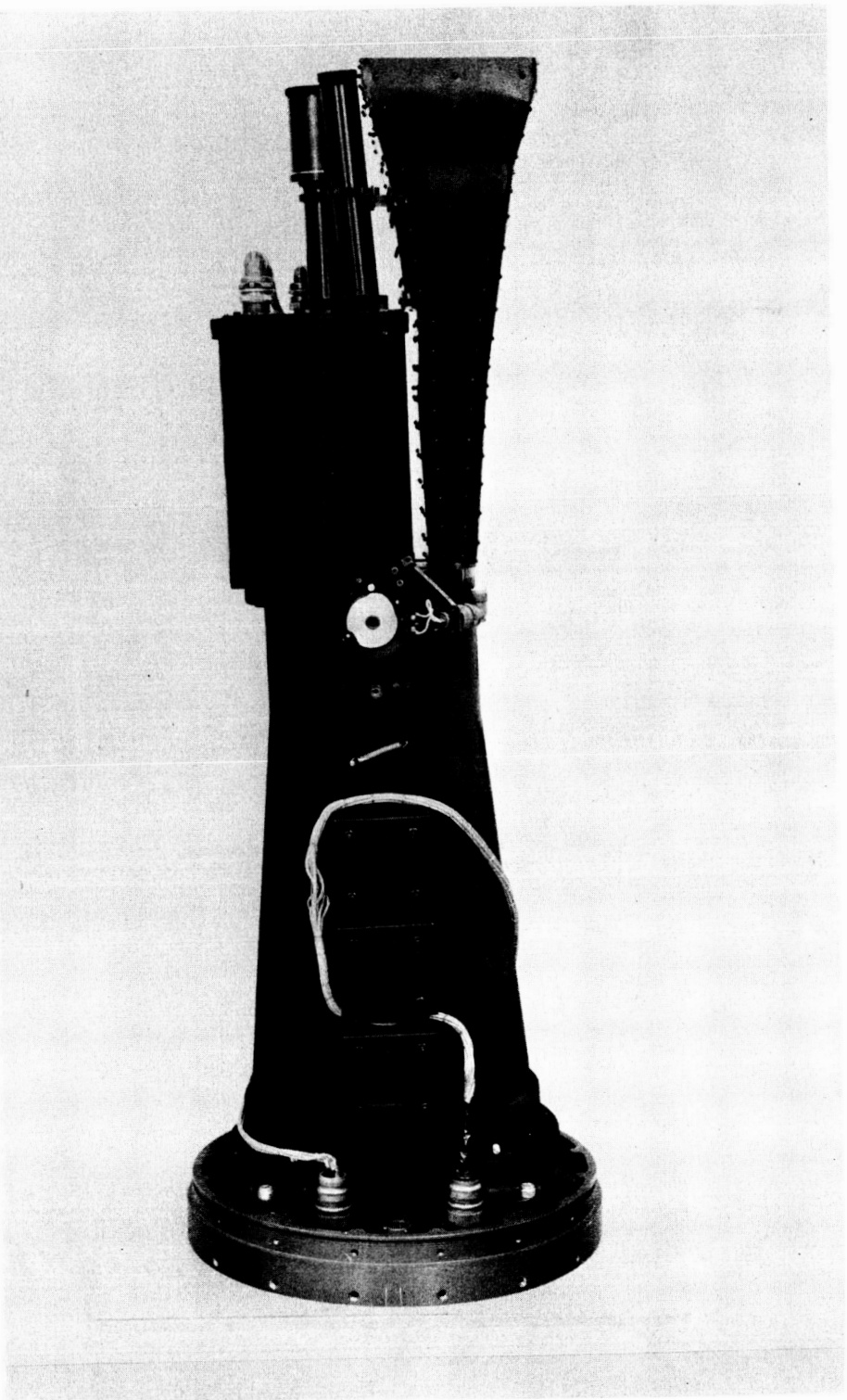

Fig. 4. Photograph of Flight Spectrometer

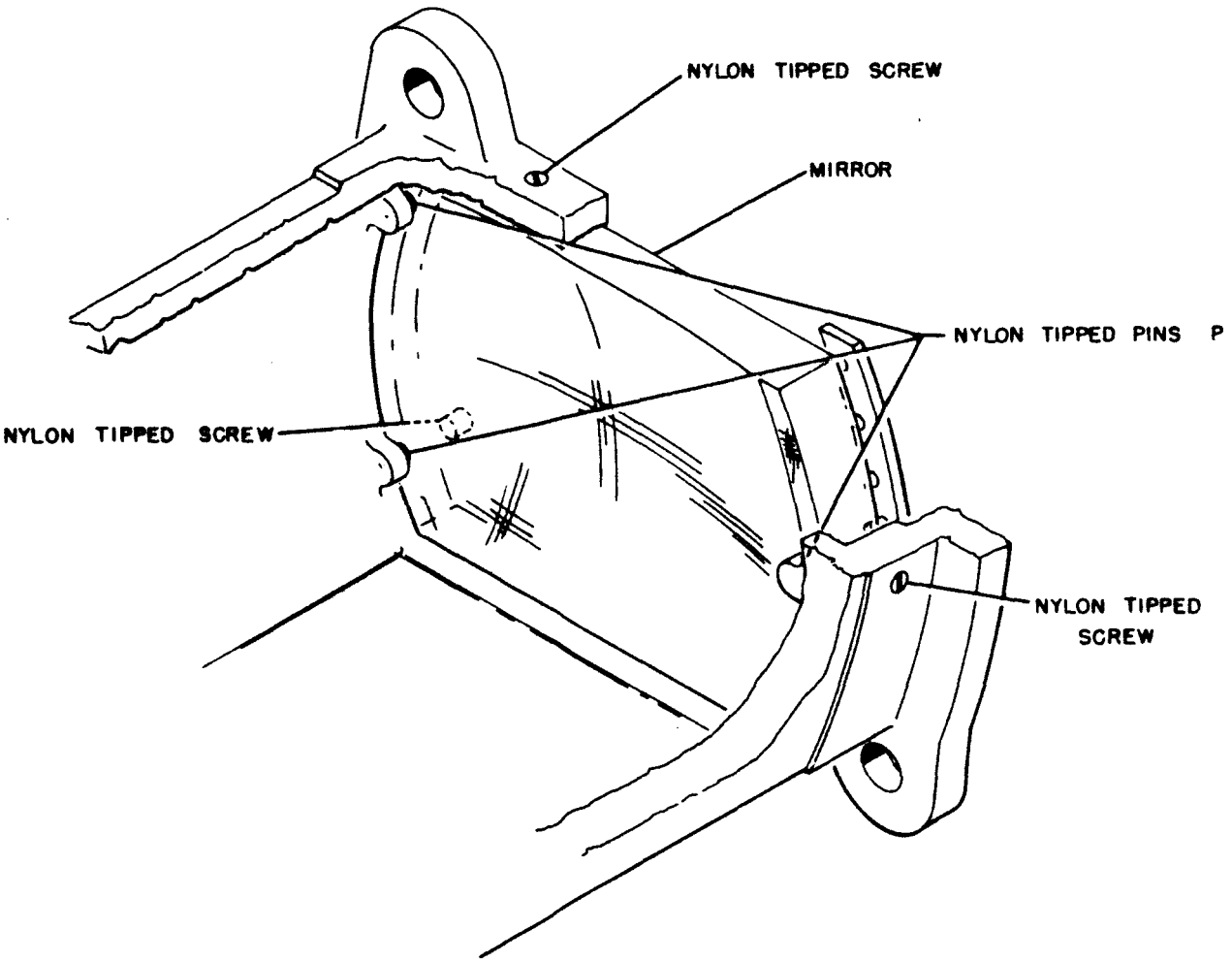

Fig. 5. Ebert Mirror Mount

The slit assembly, which fastens on the top closure plate, is shown in Fig. 6. The slit jaws are circularly curved about a point on the axis of the spectrometer. The outer jaws J_1 are fixed in position, and the inner jaws J_2 can be moved in the focal plane by rotation of the slit shaft. The drive-arm on the slit shaft can be controlled by a cam on the wavelength drive motor, and thus the slit width can be programmed with the grating position, or the slit shaft can be locked in a fixed position.

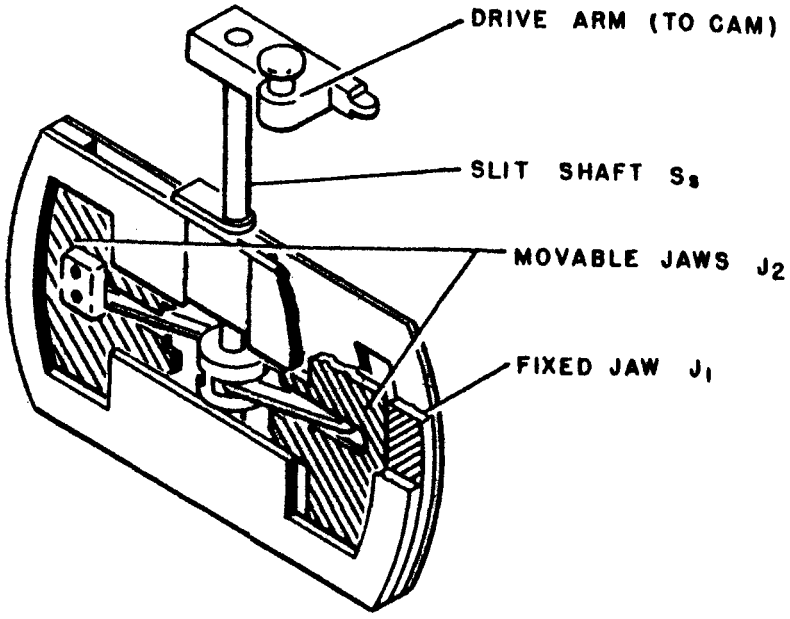

Fig. 6. Double Slit Mechanism

The details of the drive mechanism are shown in Fig. 7. The grating shaft, the motor shaft and the slit shaft are all parallel, the motor being mounted to the main housing between the grating and the slit plane. A third cam on the motor shaft operates a microswitch which shorts the output of one of the photometer channels in a coded manner to provide wavelength readout.

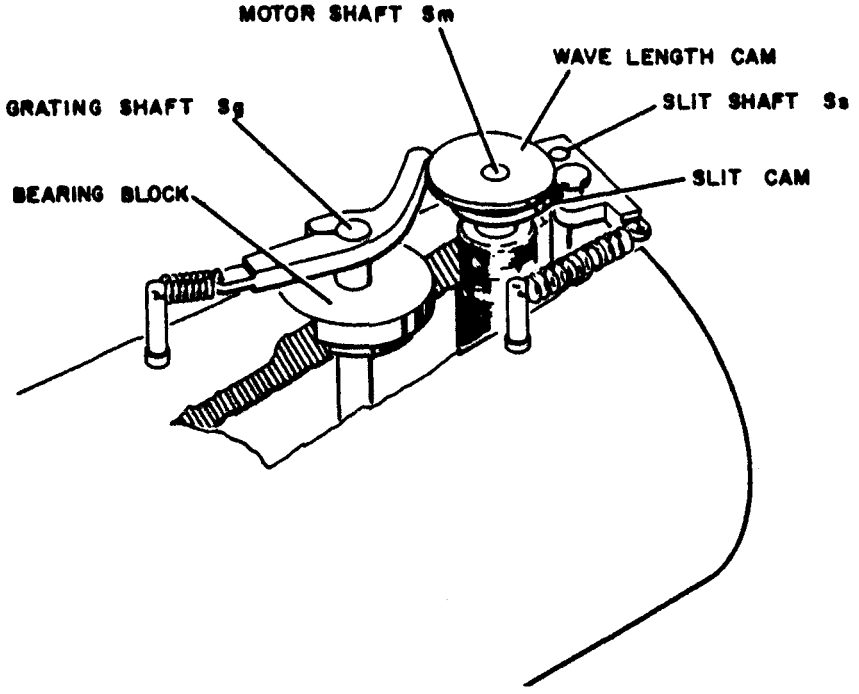

Fig. 7. Motor Cam Drive Assembly

A close-up photograph of the drive system is shown in Fig. 8.

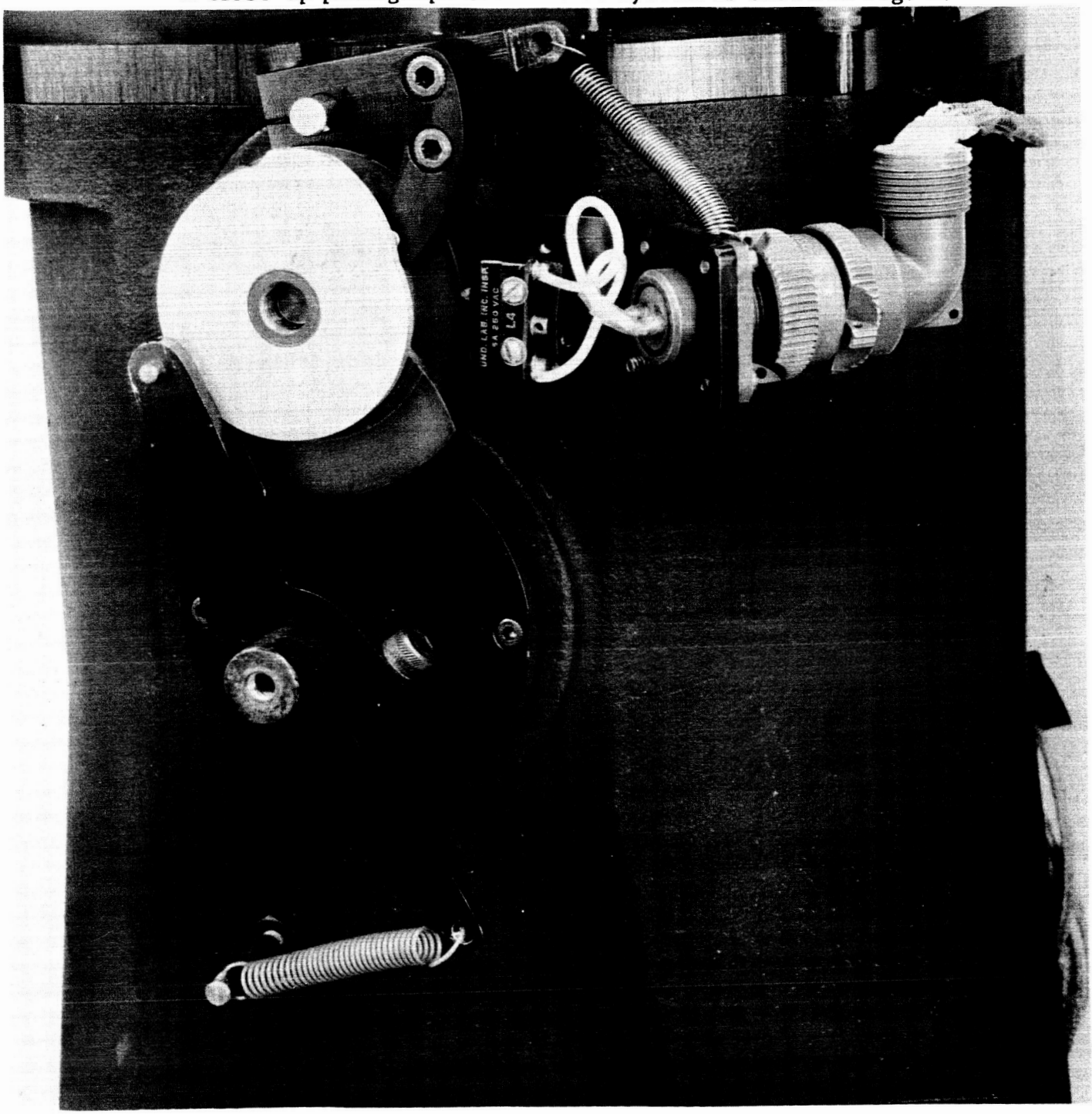

Fig. 8. Close Photograph of Drive System

The details of the detector head are shown in Figs. 9 and 10. The housing is pressurized to prevent breakdown of the high voltage circuits during flights. The face of each tube projects through the wall of the housing and is supported by a radial "O" ring between the tube wall and the housing to provide a shock support and a pressure seal.

Dayglow measurements require extremely good baffling of both the entrance slit and the filtered photometers, particularly when the measurements must be made at small angles with respect to the sun, because atmospheric emissions in selected bands can be as small as 10^{-9} of the total solar flux. To minimize the scatter from direct sunlight, we have employed double-angle baffles shown schematically in Fig. 11. The outer, larger baffle is designed to prevent direct solar radiation from reaching the inner baffle at the closest sun angle anticipated. For the photometer, therefore, only radiation scattered by the first baffle, and rescattered by the inner baffle to the detector surface can produce a false signal. In the case of the spectrometer, the false signal must again be scattered from the entrance slit to the grating.

IV. Electronic Circuitry

The high voltage device required to sensitize the photomultiplier tubes and the amplifiers to convert the tube outputs to signals which are compatible with telemetry requirements employ well-known transistor circuitry. Figs. 12, 13, 14, and 15 show the circuit for the high voltage supply, the amplifiers, and the electrical wiring diagram for the battery power supply and for the detector housing. This circuitry requires less than 2 watts to operate four photomultiplier tubes. The manner in which the battery power supply is mounted is shown in Fig. 16.

Although measurements of absolute intensity in the vacuum ultraviolet region can presently be made with limited accuracy, and the brightness measurement of weak spectral features is limited by quantum noise, the circuitry shown in Figs. 12 to 15 is capable of measuring spectral brightness to at least 1% of the full scale sensitivity of the detector. The 24 volt to 18 volt stabilizer, combined with the 18 volt to 3000 volt converter, provides a high voltage which is constant to at lease 0.1%. The operational amplifiers have been used in the full scale range 10^{-6} to 5×10^{-10} amperes with zero stability and linearity at most 1% of the range.

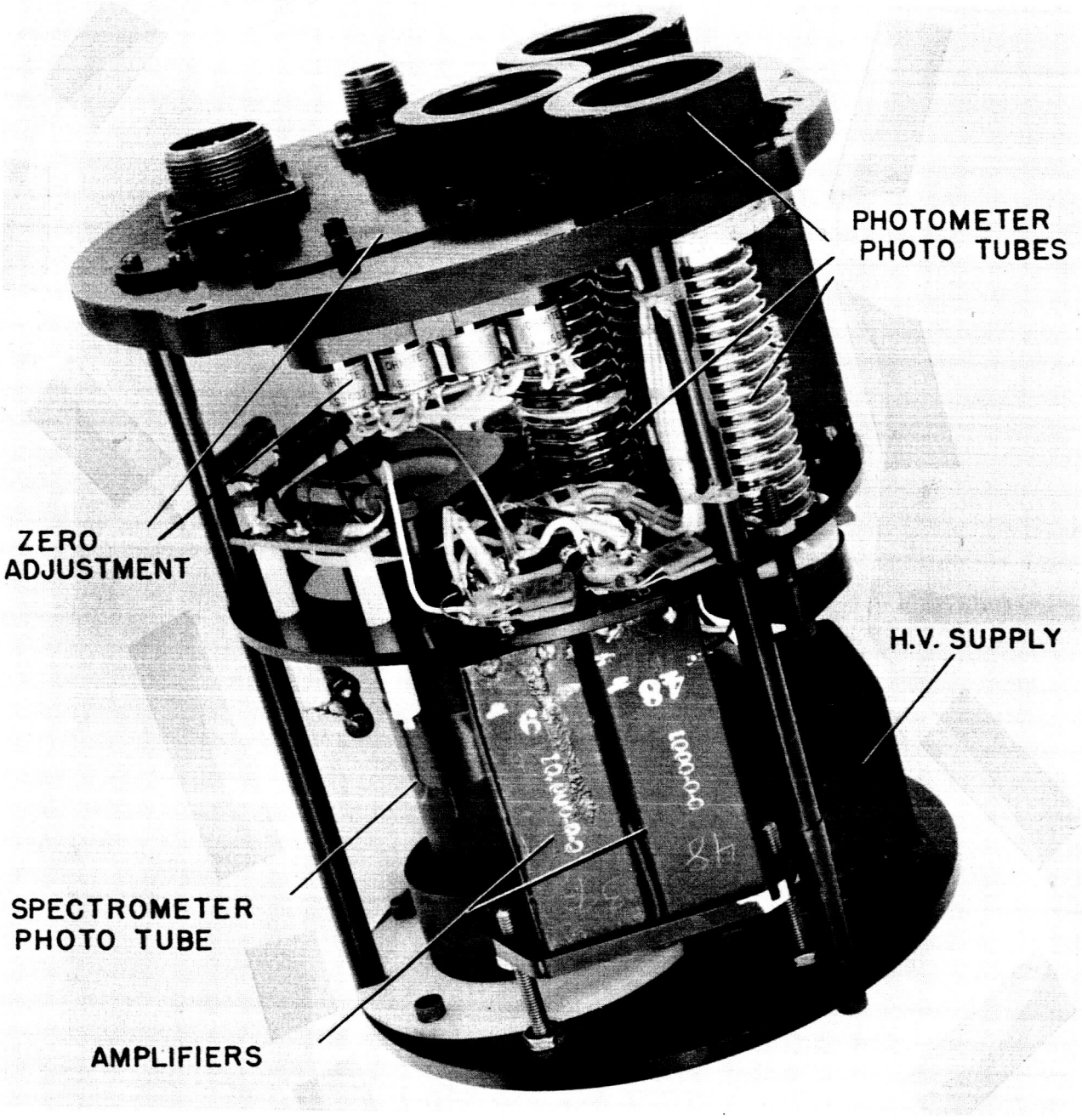

Fig. 9 Detector Head

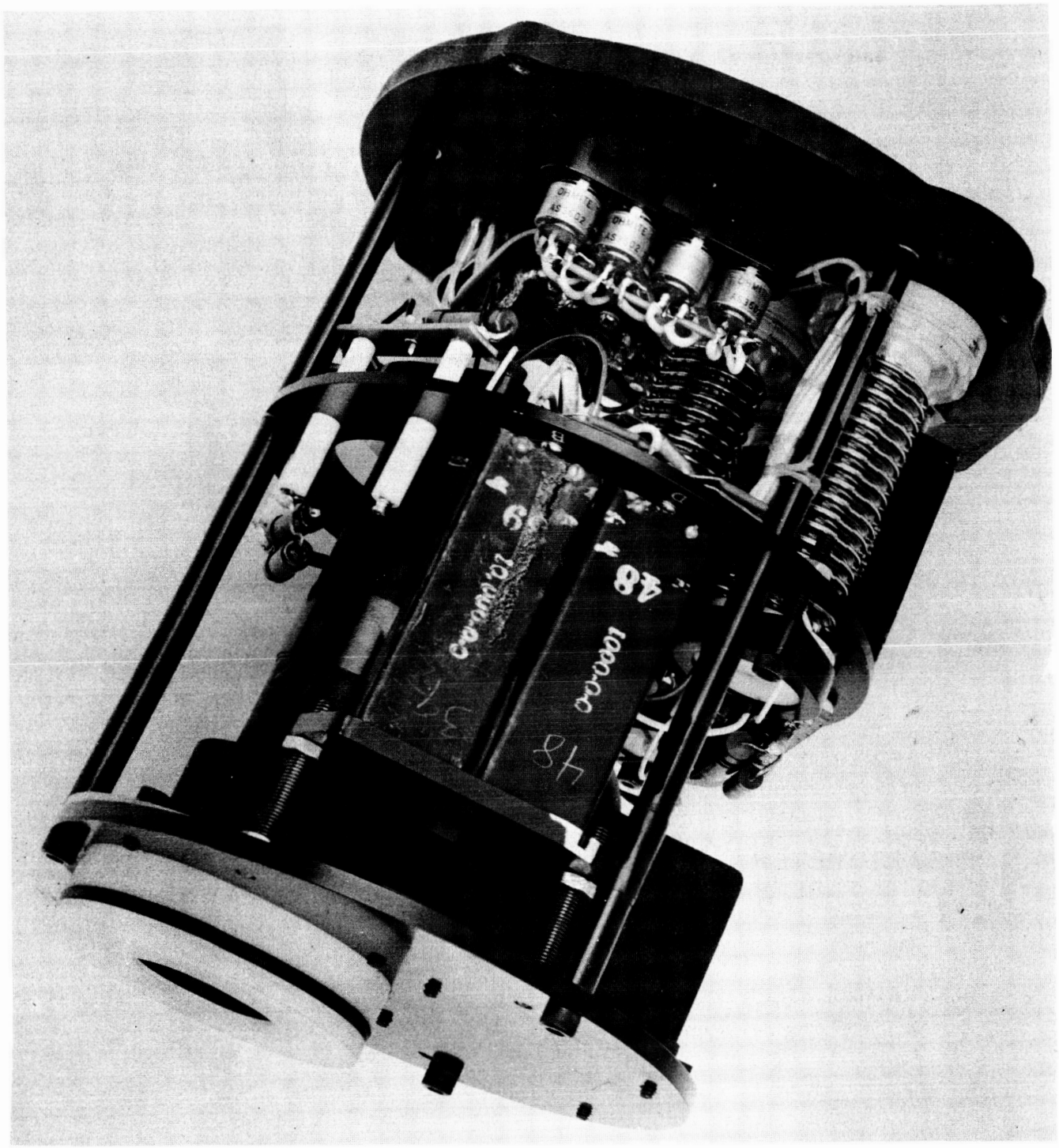

Fig. 10 Detector Head

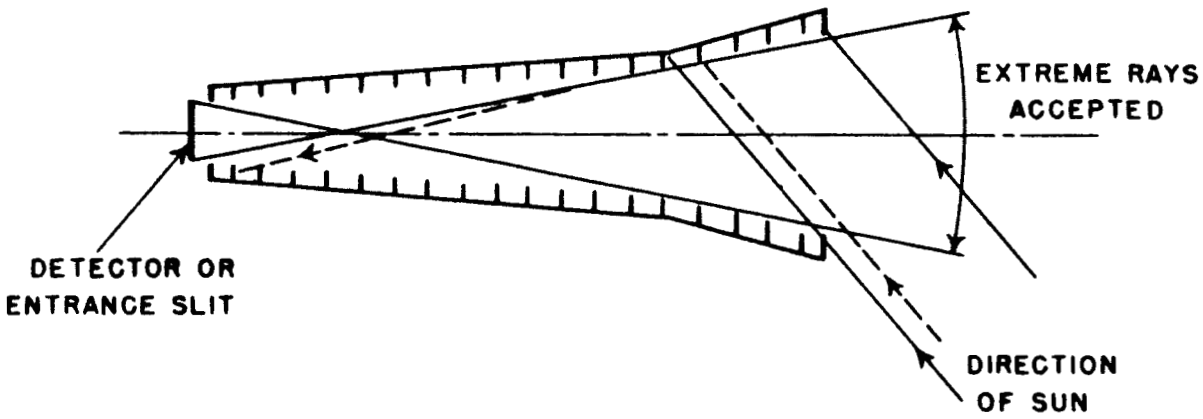

Fig. 11. Sketch of Double Baffle

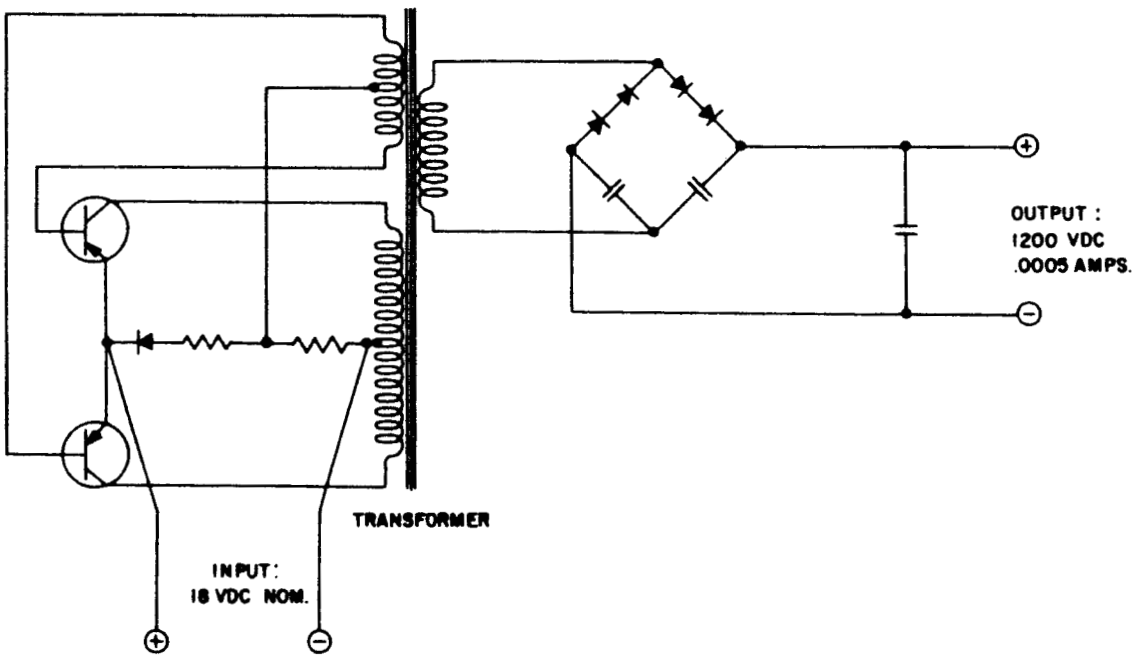

Fig. 12. High Voltage Converter for Photomultiplier Tubes

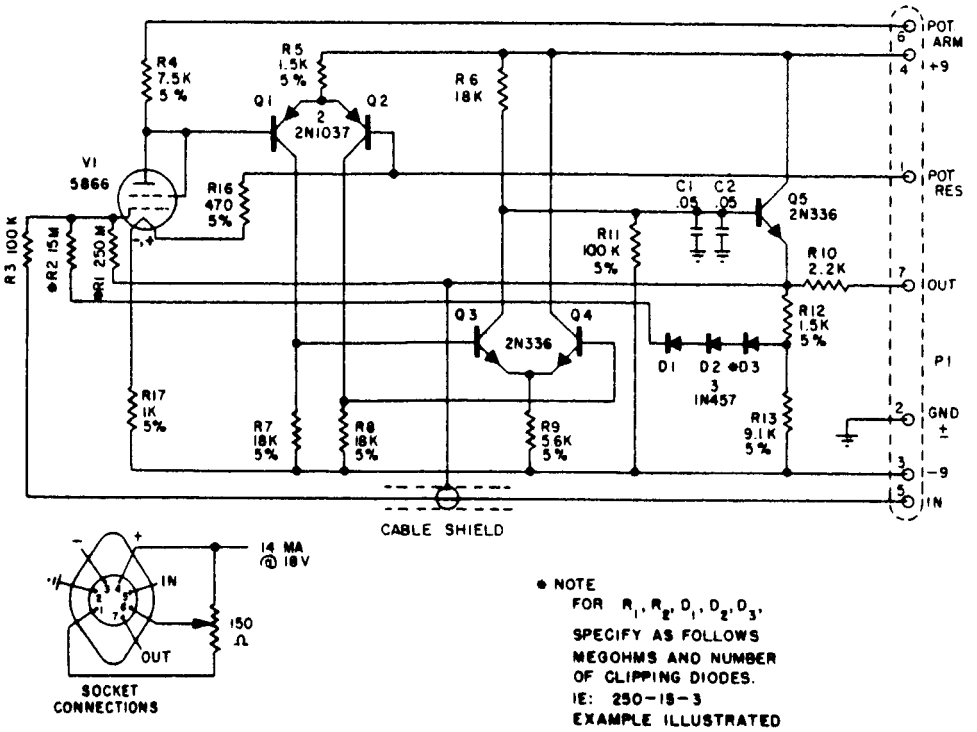

Fig. 13. Plug-In Electrometer Amplifier

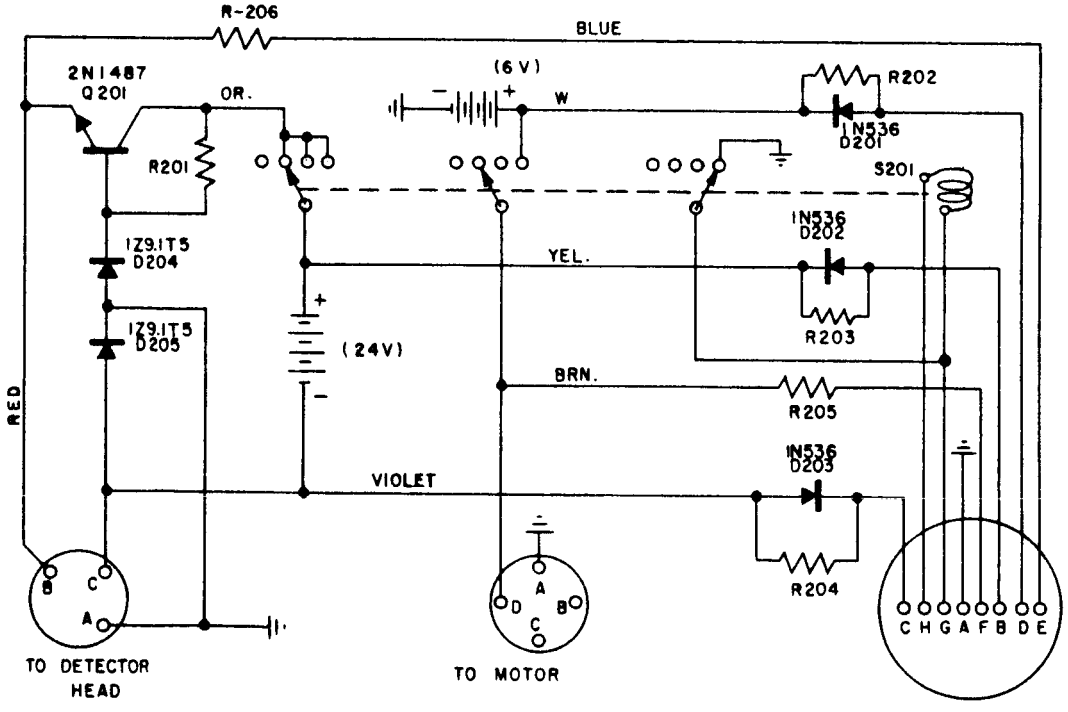

Fig. 14. Battery Box Circuitry

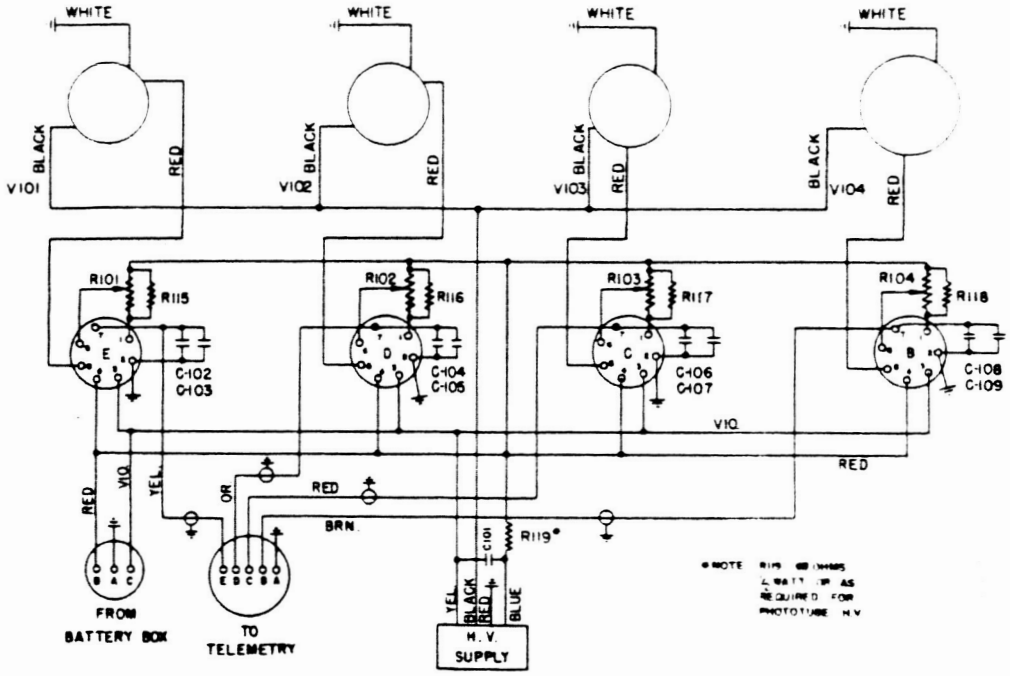

Fig. 15. Detector Head Circuitry

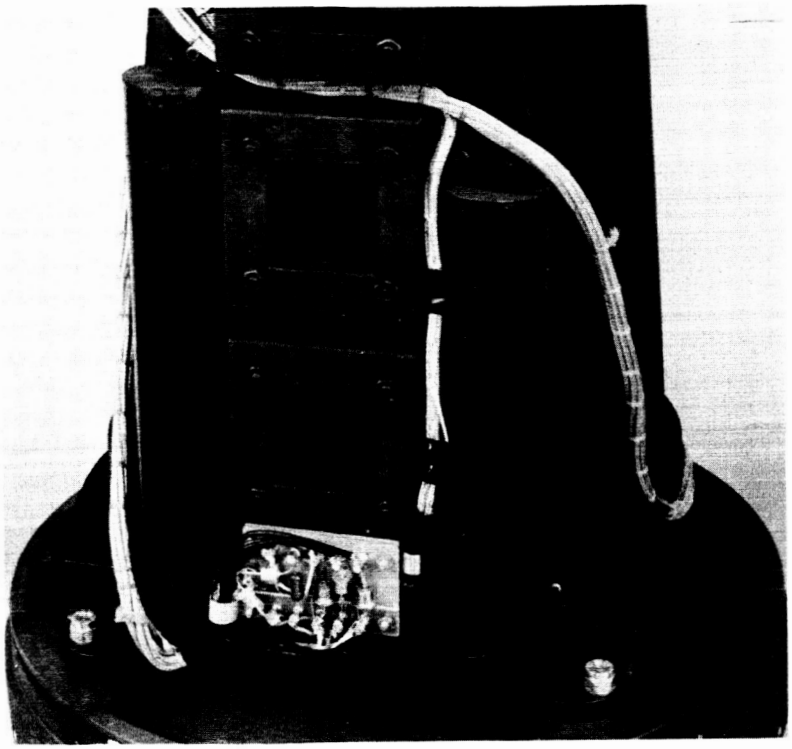

Fig. 16. Photograph of Battery Power Supply Mounting

V. Ground Based Monitor

Fig. 17 is a photograph of a flight instrument which has been adapted to ground based measurements of upper atmospheric emissions in the visible region. This instrument is equipped with a telescope and is mounted on an elevation and azimulth table. In the left background is a battery converter, in the left foreground the control box for operating the equipment, and on the right the recorder. This equipment is a completely portable, self-powered, spectrometer capable of measuring extremely weak light signals. It has been used in our program to monitor the night sky during rocket experiments on the nightglow, to study twilight emissions and aboard a Douglas DC 8 to study upper atmospheric scattering during the July 20, 1963 eclipse of the sun.

VI. Laboratory Calibration Equipment

In order to study the properties of flight spectrometers under upper atmospheric conditions, a vacuum tank has been built for testing instrument performance at low pressures. The tank is shown in the photograph of Fig. 18. The instrument can be operated while under vacuum and wavelength calibration can be accomplished in the vacuum ultraviolet with the gas discharge source shown on the right. When we have developed techniques for producing calibrated sources, the above equipment will also be useful for absolute sensitivity calibration of flight equipment.

At the present stage of development sensitivity calibration is a several step process which is accomplished with the equipment shown in Fig. 19. The unit on the left is a Jarrell-Ash Co. 1 meter Ebert spectrophotometer, which, when employed with a stable far U. V. source can be used to compare flight photomultiplier tubes against secondary standards, against a constant quantum efficiency phosphor (sodium salycilate) and against nitric oxide ionization chambers.

The black tank on the right of Fig. 18 is a second vacuum chamber in which flight optical components can be placed in the precise relative position employed in the flight instrument. With this arrangement the optical transmission of the flight optical system can be measured. The orientation of the second tank can be changed by 90^0 to determine if the transmission measurement is affected by polarization introduced by the primary monochromator.

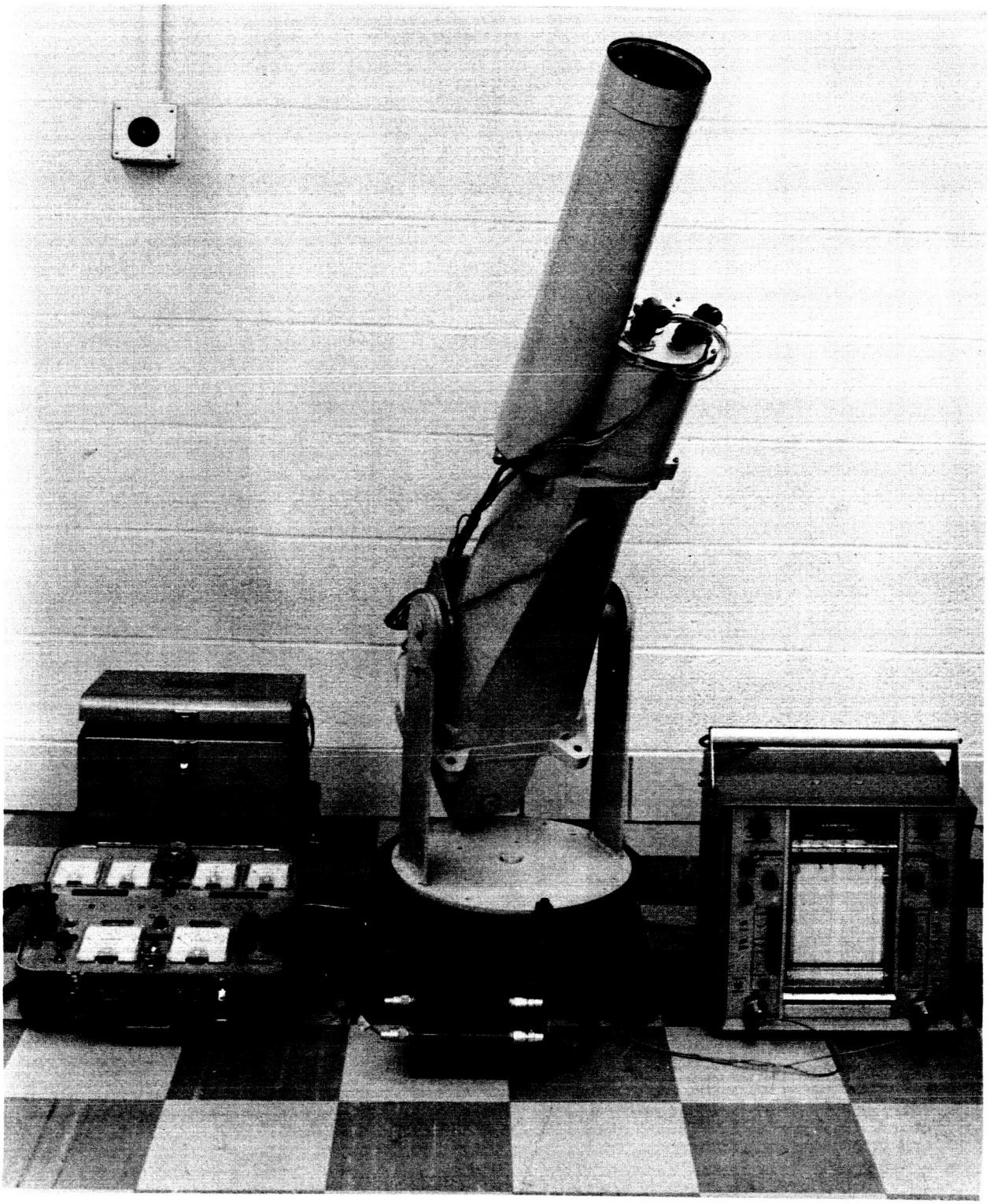

Fig. 17. Photograph of a Ground Based Monitor

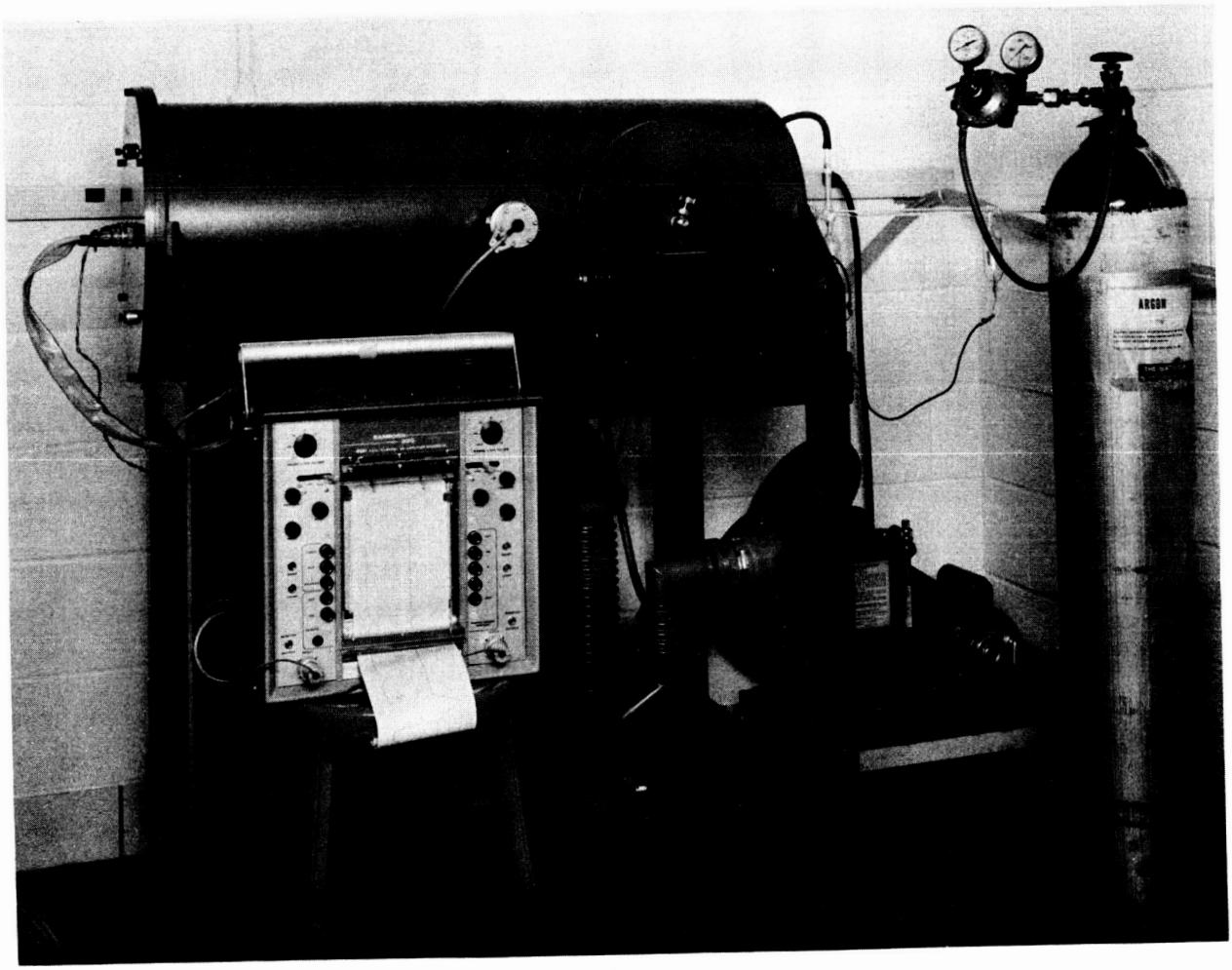

Fig. 18. Photograph of Vacuum Testing Unit.

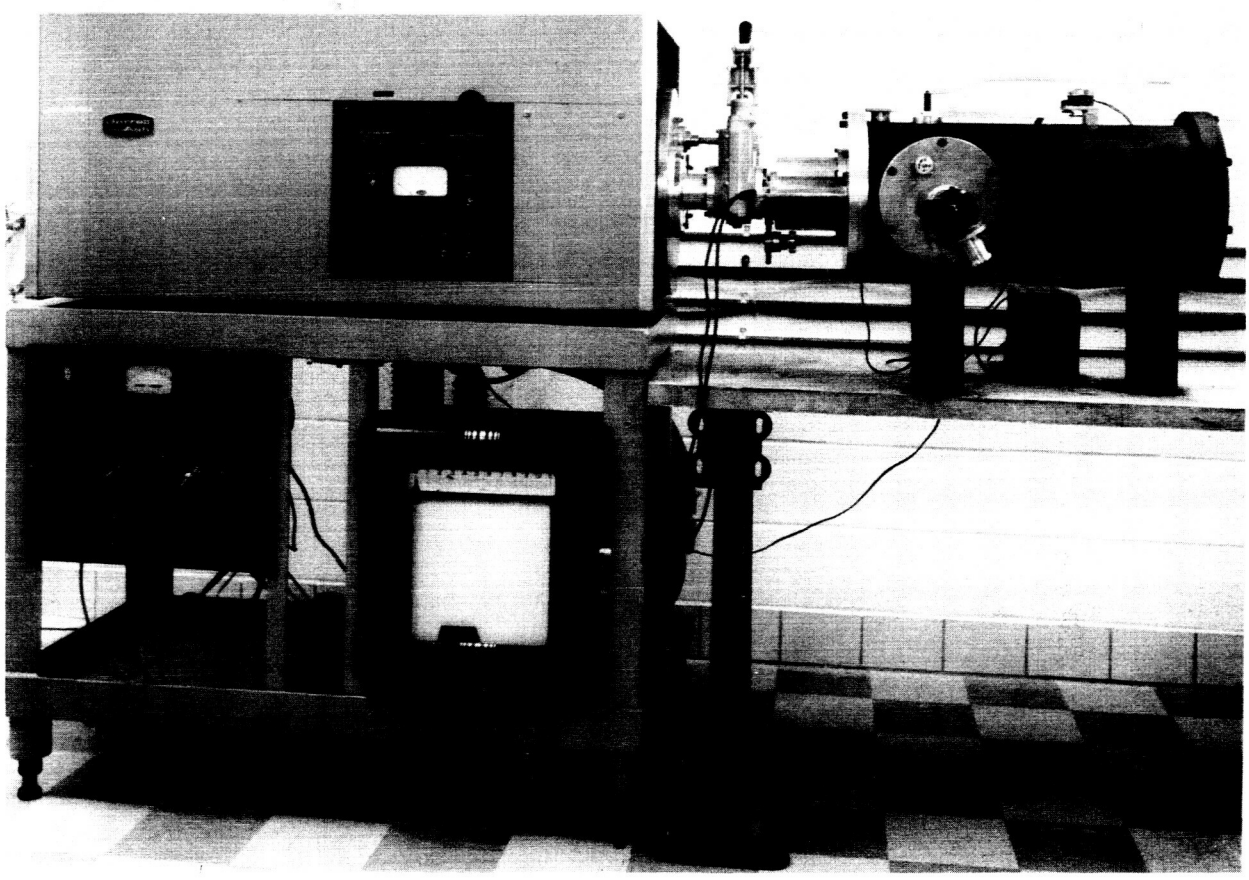

Fig. 19. Double Monochromator Calibrating Unit

VII. Conclusion

The flight instrumentation described above has been in continual evolution during the past few years, and we anticipate continued development to produce lighter, more sensitive, more precise and more flexible flight instruments for future upper atmospheric, interplanetary, planetary, and astronomical measurements. A continuing program to develop intensity standards and calibration equipment is expected to make it possible to make high precision absolute intensity measurements in the vacuum ultraviolet region.